

# Operational Characteristics of the Superconducting High Flux Plasma Generator Magnum-PSI

M.J. van de Pol, S. Alonso van der Westen, D.U.B. Aussems, M.A. van den Berg, S. Brons, H.J.N. van Eck, G.G. van Eden, H.J.W. Genuit, H.J. van der Meiden, T.W. Morgan, J. Scholten, J.W.M. Vernimmen, E.G.P. Vos and M.R. de Baar

*DIFFER – Dutch Institute for Fundamental Energy Research, De Zaale 20, 5612 AJ Eindhoven, the Netherlands*

The interaction of intense plasma impacting on the wall of a fusion reactor is an area of high and increasing importance in the development of electricity production from nuclear fusion. In the Magnum-PSI linear device, an axial magnetic field confines a high density, low temperature plasma produced by a wall stabilized DC cascaded arc into an intense magnetized plasma beam directed onto a target. The experiment has shown its capability to reach conditions that enable fundamental studies of plasma-surface interactions in the regime relevant for fusion reactors such as ITER:  $10^{23} - 10^{25} \text{ m}^{-2}\text{s}^{-1}$  hydrogen plasma flux densities at 1-5 eV for tens of seconds by using conventional electromagnets. Recently the machine was upgraded with a superconducting magnet, enabling steady-state magnetic fields up to 2.5 T, expanding the operational space to high fluence capabilities for the first time. Also the diagnostic suite has been expanded by a new 4-channel resistive bolometer array and ion beam analysis techniques for surface analysis after plasma exposure of the target. A novel collective Thomson scattering system has been developed and will be implemented on Magnum-PSI. In this contribution, the current status, capabilities and performance of Magnum-PSI are presented.

Keywords: ITER, Plasma-surface interactions, ELMs, Linear plasma device

## 1. Introduction

The plasma facing components of ITER [1], and especially its divertor, have to survive high continuous and  $\sim 1$  ms transient heat loads, of the order of  $10 \text{ MW/m}^2$  and  $1 \text{ GW/m}^2$  respectively during long exposures. These extreme conditions are unprecedented in fusion devices currently operational. In order to contribute to the study of the complex physics of plasma surface interactions (PSI) under high flux, high heat load and high fluence conditions, the Dutch Institute For Fundamental Energy Research (DIFFER) has developed the linear plasma generator Magnum-PSI. In this device, plasma is produced by a wall stabilized DC cascaded arc plasma [2] source that emits the plasma into a vacuum vessel. A strong magnet field confines the plasma into an intense plasma beam that is directed to the target surface where the plasma surface interaction takes place. The cascaded arc plasma source is chosen for its excellent performance to produce the required high hydrogen plasma flux of  $10^{23} - 10^{25} \text{ m}^{-2}\text{s}^{-1}$ , with plasma temperatures in the eV range. The cascade source can be operated in steady state as well as in pulsed mode with the help of a capacitor bank in parallel to the source DC power supply. This enables the study of power transients with similar characteristics as Edge localized Modes (ELM's), as observed in tokamaks. Because of the large fraction of neutrals emitted by the cascaded arc source due to its relatively low ionization efficiency of approximately 10%, and the need to maintain a low neutral pressure at the target, a differentially pumped vacuum vessel has been designed. The vacuum vessel is divided into three individually pumped chambers, with flow restrictions (skimmers) in between them. The skimmers block most of the neutrals,

leading to a low neutral pressure near the target, while the plasma flow can reach the target without limitation. The neutral pressure in all three vacuum chambers can be adapted to experimental requirements by varying the pump speed of the three pumps. Neutral pressure in the target region can be lower than 1 Pa during plasma exposure. This pressure is mainly caused by recombination of ions on the target. For plasma detachment studies, the pressure can be adapted not only by changing the pumping speed, but also by gas seeding into the target chamber. A superconducting magnet [3] is used to confine the plasma beam in steady-state operation, allowing for extreme high fluence studies. The targets are mounted on a water cooled, movable target holder. Both position and inclination angle of the target with respect to the plasma beam can be changed remotely. Bias can be applied to the target to vary the energy of the incoming particles.

Since September 2016, with the arrival and installation of the superconducting magnet, Magnum-PSI is now fully operational, capable of reaching its design goals. Before this, Magnum-PSI has been operated in a reduced set-up, using conventional pulsed Bitter coils, as has been described in [4]. In this contribution the current status, capabilities and performance of Magnum-PSI are presented, with a focus on steady state superconducting operation that is now available.

## 2. Design parameters

The Magnum-PSI device is designed to reach the ITER relevant regime of plasma surface interaction (PSI),

especially during the detached mode of operation of the ITER divertor. Therefore, the fundamental performance goals are stated as [1]:

- electron density  $n_e \sim 10^{19} - 10^{21} \text{ m}^{-3}$
- electron temperature  $T_e \sim 0.1 - 10 \text{ eV}$
- particle flux  $\sim 10^{23} - 10^{25} \text{ m}^{-2}\text{s}^{-1}$
- heat flux (steady state)  $> 10 \text{ MW m}^{-2}$

On top of these design parameters, additionally the following ITER relevant design choices have been made:

- low neutral background density  $< 1 \text{ Pa}$
- strong magnetic field up to 2.5 T
- cooling power of the target up to 100 kW
- high fluence (long timescale) capability
- heat flux (transient) up to  $1 \text{ GW m}^{-2}$ , with variable repetition rate up to 100 Hz

A side view of Magnum-PSI, with a quarter cut-out of the magnet to show the interior of the machine, is shown in Figure 1.

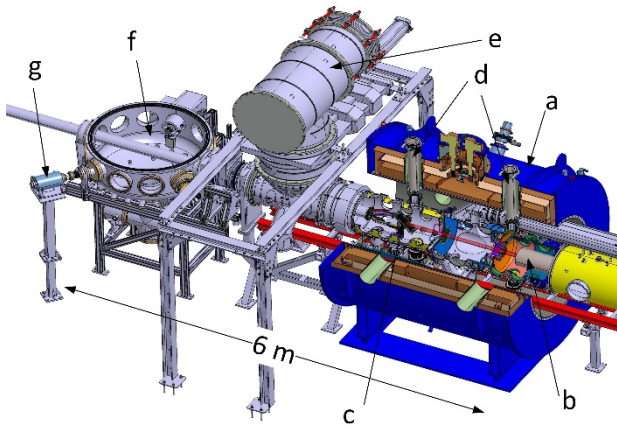


Fig. 1. A side view of Magnum-PSI, with a cut-out of the superconducting magnet. Shown are: (a) the superconducting magnet; (b) the plasma source; (c) the target at its plasma exposure position; (d) Thomson scattering laser beam tubes; (e) vacuum pumping tube; (f) Target Exchange and Analysis Chamber (TEAC); (g) part of the ion beam line, connected to the TEAC.

### 3. The superconducting magnet

In order to fulfill the required steady state capability of Magnum-PSI, a superconducting magnet [3], has been installed to magnetize and confine the plasma. It consists of 5 solenoid coils which are wound from insulated rectangular NbTi wires, with a total inductance of 492 H. The maximum current is 257 A to reach the maximum magnetic field of 2.5 T. For experimental flexibility, the magnetic field strength can be changed routinely. It can be ramped up from zero to the maximum value of 2.5 T in approximately 1 hour and 20 minutes. Field uniformity is better than  $\pm 3\%$  over a length of 1500 mm and within a cylindrical volume with radius  $\pm 100 \text{ mm}$  from the center of the coil. The magnetic stray field is passively shielded by iron walls surrounding the experimental area.

To enable good diagnostic access to study PSI physics, the bore size of the magnet is chosen to be 1250 mm. The

diagnostic ports through the magnet cryostat are installed to have direct radial lines of sight to the plasma beam and the target area. The magnet has 2 sets of 8 diagnostic ports with 174 mm inner diameter, in 2 polar planes on the longitudinal axis, with 1250 mm axial separation, and with 45 degrees angular separation. The axial location of the diagnostic ports enables viewing the plasma beam just downstream of the plasma source exit and just in front of the target. The target can be observed both tangentially and with a  $\sim 30^\circ$  angle with respect to the field axis of the magnet, perpendicular to the target. The total size of the magnet is  $3.1 \times 2.8 \times 2.6 \text{ m}$  (height  $\times$  length  $\times$  diameter), and it weighs about 15000 kg. The magnet is shown in Figure 2.

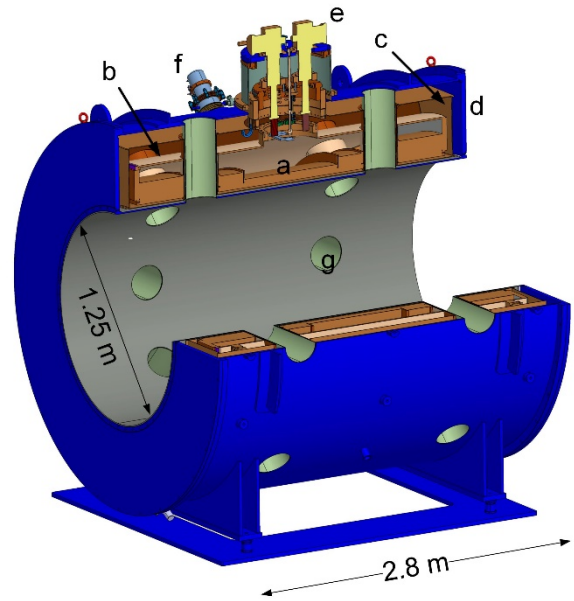


Fig 2. A cut-out of the superconducting magnet of Magnum-PSI, showing its interior structure: coils (a), helium vessel (b), radiation shield (c) and vacuum vessel (d). The Sumitomo recondensator cold heads (yellow parts in the figure) are installed at the turret (e). The Leybold radiation shield cold head is depicted at (f). The diagnostic ports (g), and a few typical dimensions of the magnet are shown.

The magnet system consists of a winding body, on which the NbTi wires are wound, placed inside a 1600 liter liquid helium vessel, surrounded by a radiation shield, inside a vacuum vessel. To decrease radiation losses, the surfaces of the helium vessel and the radiation shield are wrapped with superinsulation (Coolcat 2NW multilayer insulation). Most electrical and cryogenic connections are located in the turret on top of the cryostat.

The cooling system is designed as a zero boil-off system with permanently connected High Temperature Superconductor (HTSC) current leads. The evaporated liquid helium is re-condensed by two 2-stage Sumitomo RDK-415D cold heads and a Cryomech Helium Re-Liquefier (HeRL45) system equipped with three cold heads. The total re-liquefying power is 7.5 W. In addition, the thermal shield is cooled by a Leybold Coolpower MD250 cold head. Zero boil-off has been achieved both in steady-state operation with constant magnetic field, and during ramp-up and ramp-down of the magnetic field.

## 4. Diagnostics

One of the essential design criteria for Magnum-PSI is to enable access for an extensive set of plasma and surface diagnostics. The surface diagnostics include techniques to measure surface properties during plasma exposure of the target, and techniques to determine the properties of the target surface after the interaction with the plasma. For the application of the latter techniques, the target can be retracted under vacuum to the Target Exchange and Analysis Chamber (TEAC), for enhanced diagnostic access.

### 4.1 Thomson scattering diagnostics

Incoherent Thomson Scattering (TS) is the key plasma diagnostic to measure both  $n_e$  and  $T_e$  profiles along the laser chord perpendicular to the plasma beam [5]. This can be done at two locations: close to the plasma source exit, and in front of the target. The detection system measures the scattered light at 50 spatially distributed positions along a laser chord of 95 mm, with a spatial resolution of 2 mm. The minimum measurable  $n_e$  and  $T_e$  are  $\sim 1 \times 10^{17} \text{ m}^{-3}$  and  $\sim 0.07 \text{ eV}$ . The accuracy of the  $n_e$  and  $T_e$  measurement is 3% and 6% respectively at  $n_e = 9.4 \times 10^{18} \text{ m}^{-3}$ , obtained by averaging of 30 laser pulses (0.6 J, 10 Hz). Single pulse TS yields the same accuracy for  $n_e > 2.8 \times 10^{20} \text{ m}^{-3}$ , with a maximum repetition rate of 5 Hz, set by the read-out speed of the ICCD camera. Single pulse TS has been applied successfully at Magnum-PSI during transient heat load experiments. A collective Thomson Scattering (CTS) system is being implemented on Magnum-PSI [6]. CTS shows the collective motion of the electrons, bunched in the Debye sphere of the ions, rather than the individual motion of the electrons, as in incoherent TS. Therefore the ion temperature  $T_i$  and the plasma velocity  $v_{\text{plasma}}$  can be measured, both with a high accuracy of  $< 8\%$  and  $< 15\%$ , respectively. The concept of CTS has been tested successfully at Pilot-PSI, the forerunner of Magnum-PSI.

### 4.2 Spectroscopic diagnostics

Wide spectral range optical emission spectroscopy (OES) is applied to measure impurity concentrations in the plasma in front of the target. A fast visible light camera (Phantom), with a frame rate of up to 1 MHz, is available to measure fast phenomena near the surface, e.g. droplets emitted from liquid metal surfaces, or the effect of dust particles in the plasma.

To measure recombination radiation and emission by impurities in the near surface plasma region, a novel 4-channel resistive foil bolometer has been installed [7]. The bolometer views the plasma radiation perpendicular to the beam axis, over an axial length of  $\sim 50 \text{ mm}$ , centered at the TS measurement position. The total near-surface plasma emissivity can be measured by moving the target into view of the bolometer. Each channel has a spatial resolution of  $\sim 10 \text{ mm}$  axially, and  $\sim 12.8 \text{ mm}$  radially, when the sensor is at the smallest distance from the viewing aperture. The distance between sensor and aperture can be increased by a translation manipulator,

thereby decreasing the solid angle of the received radiation while increasing the spatial resolution. The heat absorber, with a size of  $3.94 \times 1.4 \text{ mm}^2$ , has a noise-equivalent power density of  $\sim 20 \mu\text{W}/\text{cm}^2$ . To enhance the absorption of the sensor in the visible spectrum, where a significant part of the radiated power loss in Magnum-PSI will occur, 2 out of the 4 channels have been coated with a thin carbon film.

### 4.3 Surface analysis diagnostics

During plasma exposure, the target's surface temperature is measured in 2D by a fast infrared camera (FLIR SC7500-MB) with a maximum frame rate of 30 KHz, and by a single-point multi-wavelength spectroscopic pyrometer (FAR Spectro Pyrometer model FMPI). The pyrometer is used also for in-situ calibration of the infrared camera. Temperature and flow sensors are installed on the water cooling circuits of the target holder to determine the total heat load on the target by calorimetry.

For analysis of the targets after plasma exposure, laser and ion beam diagnostics are installed on the TEAC. Laser Induced Breakdown Spectroscopy (LIBS) is being developed for surface composition measurements. Using the ions produced by a 3 MeV singletron accelerator, several surface analyses techniques can be employed. Currently available are Rutherford Backscattering Spectroscopy (RBS), for the detection of  $Z > 1$  elements and Nuclear Reaction Analysis (NRA). Elastic Recoil Detection (ERD) is currently being commissioned. Both NRA and ERD have detection capability for  $Z < 17$  elements. All these techniques can be applied to investigate target properties quickly after plasma exposure, without exposing the targets to atmospheric conditions in between. This is accomplished by the translation of the target under vacuum from the exposure position inside the magnet bore to the TEAC.

## 5. Operational characteristics

Magnum-PSI can produce a wide range of plasma parameters by setting the gas flow, plasma source current, magnetic field strength, target bias voltage, and the three pumping speeds. Figure 3 and 4 show that for a hydrogen plasma, both the peak  $n_e$  and  $T_e$  value increase with magnetic field strength  $B$ . The increase of plasma source cathode current yields a higher  $n_e$  but a lower  $T_e$ . An increase of gas flow, while the pumping speed is kept constant, decreases  $T_e$  but has only a small effect on  $n_e$ .

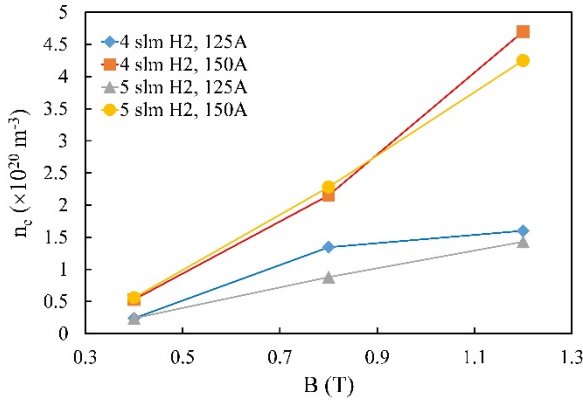


Fig. 3: Dependence of the peak value of  $n_e$  on magnetic field  $B$ , for two values of the plasma source cathode current (125 and 150 A) and two gas flows (4 and 5 standard liter per minute  $H_2$ ).

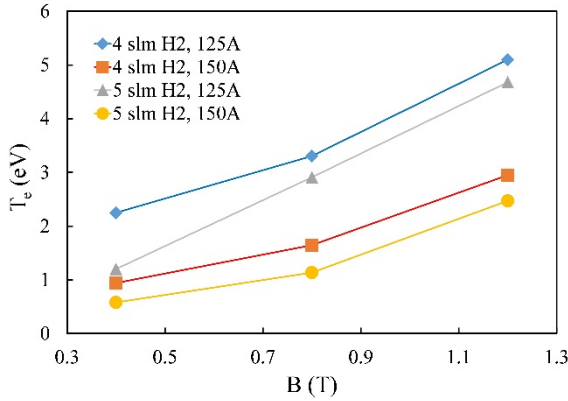


Fig. 4: Dependence of the peak value of  $T_e$  on magnetic field  $B$ , for two values of the plasma source cathode current (125 and 150 A) and two gas flows (4 and 5 standard liter per minute  $H_2$ ). The color coding is the same as in Figure 3.

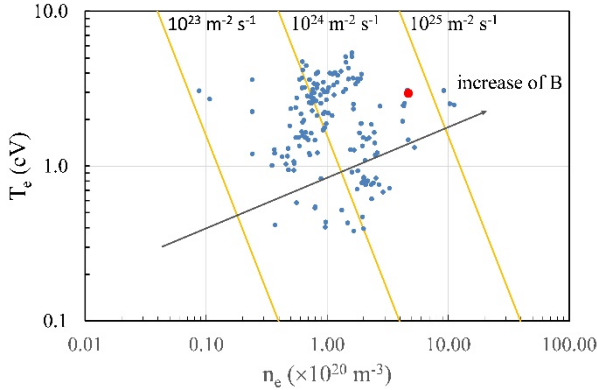


Fig. 5: Parameter space of Magnum-PSI with superconducting magnet, represented by the electron density and temperature measured with Thomson Scattering in front of the target. All points are for hydrogen plasma, without target bias. Magnetic fields up to 1.6 T have been used. Lines of constant flux are indicated by the yellow solid lines. The arrow indicates the trend of  $n_e$  and  $T_e$  with increase of magnetic field  $B$ .

In Figure 5, an overview is given of the electron density  $n_e$  and temperature  $T_e$  measured during the first few months of commissioning and experiments on Magnum-PSI with the superconducting magnet installed. All depicted measurements are for hydrogen plasmas, without target bias, and for magnetic fields up to 1.6 T. For reference, lines of constant flux are shown as the solid

diagonal lines. The obtained plasma parameters are in the range of the design values of Magnum-PSI:  $n_e \sim 10^{20} - 10^{21} \text{ m}^{-3}$  and  $T_e \sim 1 - 5 \text{ eV}$ , resulting in a particle flux of  $\sim 10^{24} - 10^{25} \text{ m}^{-2} \text{ s}^{-1}$ . The particle flux has been calculated from the measured  $n_e$  and  $T_e$  according to the Bohm criterium, where the density at the sheath edge is taken to be half of the upstream value [8]. Assuming a 2D-Gaussian plasma beam, half of the total power is contained within the full width half maximum (FWHM) area of the intensity profile. The beam intensity is proportional to  $n_e T_e^{3/2}$ . Because the measured  $n_e$  profiles are usually narrower than the  $T_e$  profiles, as is shown for a typical case in Figure 6, the FWHM of the intensity profile is mainly determined by the  $n_e$  profile. The average heat flux of the plasma beam within the FWHM of the beam can then be estimated to equal half of the total power measured by target calorimetry, divided by the FWHM area of the  $n_e$  profile. Both total power and FWHM depend on the applied magnetic field: for higher fields (while other parameters like plasma source current and gas flow remain the same), the plasma beam becomes narrower (the FWHM of the  $n_e$  profile decreases), and both  $n_e$  and  $T_e$  increase. Therefore the heat flux increases with applied magnetic field. Typical values of the average heat flux found, are  $\sim 10$ ,  $\sim 4$  and  $\sim 1 \text{ MW m}^{-2}$  for magnetic field strengths of 1.2, 0.8 and 0.4 T respectively, and a gas flow of 4 slm (standard liter per minute;  $1 \text{ slm} = 1.689 \text{ Pa m}^3 \text{ s}^{-1}$ )  $H_2$  and a plasma source cathode current of 125 A. The peak heat flux will be higher since both  $n_e$  and  $T_e$  will be higher in the center of the beam. The heat flux values are in the ITER divertor relevant regime.

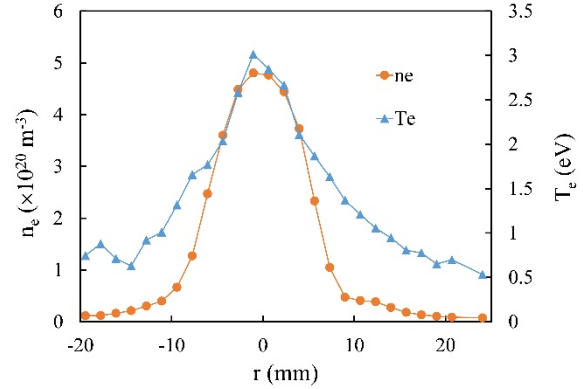


Fig. 6: Typical example of an electron density and electron temperature profile, measured by Thomson scattering, for 4 slm  $H_2$  gas flow, 150 A plasma source cathode current and a magnetic field of 1.2 T.

Although the operational range in terms of  $n_e$  and  $T_e$ , is similar to that reported for the Magnum-PSI set-up with Bitter coils instead of the superconducting magnet [3], it was obtained with significantly lower plasma source current. Now, a current between 100 and 160 A has been used, while previously 200 to 250 A was needed to reach similar results. The main causes of this reduction in the current set-up are the homogeneous, non-expanding magnetic field, and the lower neutral background pressure due to the upgrade from two- to three-stage differential pumping. The lower plasma source input power dramatically increases the life time of the plasma source.

Because of the steady-state performance of the superconducting magnet, long duration target exposures and high fluence experiments are now available on Magnum-PSI. The divertor fluence of ITER, accumulated over its lifetime, is expected to be in the  $\sim 10^{30} - 10^{31} \text{ m}^{-2}$  range. With the  $\sim 10^{25} \text{ m}^{-2}\text{s}^{-1}$  flux at Magnum-PSI, a fluence of  $10^{30} \text{ m}^{-2}$  can be reached in approximately 30 hours of exposure, making lifetime tests of plasma facing components of the ITER divertor possible in a manageable timeframe. High fluence (long target exposure) experiments on Magnum-PSI have started recently. So far the longest exposure lasted 6.5 hours. With a particle flux of  $\sim 10^{24} \text{ m}^{-2} \text{ s}^{-1}$  in this particular experiment, this corresponds to a fluence of more than  $2 \times 10^{28} \text{ m}^{-2}$ . For these extremely long, high fluence exposures, the purity of the plasma beam is of highest importance to avoid accumulation of unintended contamination of the target. Target contamination can be minimized by careful selection of the material of the target clamping components, especially in experiments with target biasing, where sputtering of the clamping material may be a source of contamination.

## 6. Outlook and conclusions

So far, Magnum-PSI has not been pushed to the limits of its operational regime. The maximum magnetic field employed was 1.6 T. A further increase towards the maximum of 2.5 T is likely to increase peak  $n_e$  and  $T_e$  values, and the average and peak particle and heat flux within the plasma beam. Operation with fields  $> 1.6\text{T}$  still needs to be commissioned. Also the plasma source has been used conservatively.

The design parameters have been achieved, without full exploration of Magnum-PSI's parameter space. This achievement, and the wide range of diagnostics, make Magnum-PSI well suited as a facility for PSI research for ITER and fusion devices beyond ITER. Current research topics for experiments on Magnum-PSI include plasma surface detachment, transient ELM-like PSI, liquid metals and vapor shielding, and deuterium retention at extremely high fluence.

## Acknowledgments

DIFFER is part of the Netherlands Organisation for Scientific Research (NWO). The work has been carried out within the framework of the EUROfusion Consortium and has received funding from the Euratom research and training programme 2014-2018 under grant agreement No 633053. The views and opinions expressed herein do not necessarily reflect those of the European Commission. DIFFER is a partner in the Trilateral Euregio Cluster TEC.

## References

[1] R.A. Pitts et al, Physics basis and design of the ITER plasma-facing components, *Journal of Nuclear Materials*,

- 415 (2011), S957
- [2] W.A.J. Vijvers et al, Experimental and theoretical determination of the efficiency of a sub-atmospheric flowing high power cascaded arc hydrogen plasma source, *Plasma Sources Sci. Technol.*, 19 (2010) 065016
- [3] H.J.N. van Eck et al, A 2.5 T, 1.25 m free bore superconducting magnet for the Magnum-PSI linear plasma generator, *IEEE Trans. Appl. Supercond.* 28 (2018) 1-5
- [4] H.J.N. van Eck et al, Operational Characteristics of the high flux plasma generator Magnum-PSI, *Fusion Eng. Des.* 89 (2014) 2150-2154
- [5] H.J. van der Meiden et al, Advanced Thomson scattering system for high-flux linear plasma generator, *Rev. Sci. Instrum.* 83 (2012) 123505
- [6] H.J. van der Meiden et al, Collective Thomson scattering system for determination of ion properties in a high flux plasma beam, *Appl. Phys. Lett.*, 109 (2016) 261102
- [7] G.G. van Eden et al, Measurements of radiated power loss in the Magnum-PSI linear plasma device using resistive bolometry, in preparation for *Nucl. Fusion*.
- [8] P.C. Stangeby, *The Plasma Boundary of Magnetic Fusion Devices*, Taylor & Francis group, London, 2000